J Mater Sci: Mater Med (2011) 22:1873–1884
DOI 10.1007/s10856-011-4374-8

Poly(lactide-co-glycolide)/hydroxyapatite nanofibrous scaffolds fabricated by electrospinning for bone tissue engineering

Lihong Lao · Yingjun Wang · Yang Zhu · Yuying Zhang · Changyou Gao

Received: 30 September 2010 / Accepted: 6 June 2011 / Published online: 18 June 2011

Abstract Poly(lactide-co-glycolide) (PLGA) nanofibrous composite scaffolds having nano-hydroxyapatite particles (HAp) in the fibers were prepared by electrospinning of PLGA and HAp with an average diameter of 266.6 ± 7.3 nm. Microscopy and spectroscopy characterizations confirmed integration of the crystalline HAp in the scaffolds. Agglomerates gradually appeared and increased on the fiber surface along with increase of the HAp concentration. In vitro mineralization in a 5 × simulated body fluid (SBF) revealed that the PLGA/HAp nanofibrous scaffolds had a stronger biomineralization ability than the control PLGA scaffolds. Biological performance of the nanofibrous scaffolds of the control PLGA and PLGA with 5 wt% HAp (PLGA/5HAp) was assessed by in vitro culture of neonatal mouse calvaria-derived MC3T3-E1 osteoblasts. Both types of the scaffolds could support cell proliferation and showed sharp increase of viability until 7 days, but the cells cultured on the PLGA/5HAp nanofibers showed a more spreading morphology. Despite the similar level of the cell viability and cell number at each time interval, the alkaline phosphatase secretion was significantly enhanced on the PLGA/5HAp scaffolds, indicating the higher bioactivity of the as-prepared nano-HAp and the success of the present method for preparing biomimetic scaffold for bone regeneration.

Electronic supplementary material The online version of this article (doi:10.1007/s10856-011-4374-8) contains supplementary material, which is available to authorized users.

L. Lao · Y. Wang · Y. Zhu · Y. Zhang · C. Gao (✉)
MOE Key Laboratory of Macromolecular Synthesis and Functionalization, Department of Polymer Science and Engineering, Zhejiang University, Hangzhou 310027, China
e-mail: cygao@mail.hz.zj.cn

1 Introduction

Bone is an organic–inorganic complex tissue composed of collagen fibers and mineral apatite [1, 2]. When slight loss or damage occurs, as a renewable tissue it can spontaneously self-repair and regenerate [3, 4]. However, bone grafts such as autografts, allografts and xenografts are still necessarily used to fill in the defects caused by trauma or disease, which are standard therapy strategies in clinic [2, 5]. A tissue engineering strategy involving the combination of cells, biomaterial scaffolds and other bioactive agents has emerged as a new approach in bone regeneration [6, 7]. The scaffold serves as an initial structure to retain the cells in the defects and to support the cell growth and phenotype maintenance, thus playing an important role in bone regeneration.

Various technologies have been developed to fabricate three-dimensional (3D) porous scaffolds [8], of which electrospinning has been proven to be a simple and versatile technology for producing ultrathin non-woven fibers with a diameter ranging from nanometers to microns [9, 10]. The electrospun nanofibers possess a lot of advantages such as an extremely high surface-to-volume ratio, a small interfibrous pore size with tunable porosity as well as vast possibilities for achieving desirable properties and functionalities, thus have been widely used in areas of filtration [11], composite reinforcements [12], optical and chemical technologies [13], drug delivery [14] and tissue engineering [9, 10]. A variety of materials including polymers, ceramics and their composites can be electrospun into fibrous scaffolds [15, 16]. However, considering the requirements of biomimetic structure, good mechanical strength and bioactivity, synthetic degradable polyesters including polylactide (PLA) and polyglycolide (PGA) are usually used as the scaffold matrix and could be further integrated with

inorganic minerals [6, 7, 17, 18]. The poly(L-lactide) (PLLA) and poly(D-lactide) (PDLA) require at least 24 months and 12–18 months to finish the degradation, respectively, while the PGA is completely degraded only after 6–12 months [8, 19]. Therefore, their copolymer, poly(lactide-co-glycolide) (PLGA), is more prospective for tissue engineering, since its mechanical properties, biodegradation products and time can be manipulated by controlling the ratio of lactide (LA) to glycolide (GA), and thereby is flexible for the clinical applications [19, 20]. Indeed, PLGA is currently widely used as scaffold materials for bone repair with good biocompatibility, non-toxicity and non-inflammation [21, 22].

Hydroxyapatite (HA) is among the family of calcium phosphate-based bioceramics [23, 24]. Due to its non-toxicity, bioactivity and osteoconductivity, and similarity of its chemical and crystalline structures as the nature bone minerals [2], the HA particles are also frequently applied solely or as a major component of the bone repair biomaterials. The nano-sized HA can improve the mechanical properties and support calcium and phosphate delivery after implantation as well. Therefore, incorporation of the nano-HA into polymer matrix is assumed to mimic the nature bone structure as well as enhance cell growth and response [25]. Together with the advantages of synthetic biopolymers, compounding of the biopolymers and HA is one of the supreme methods for obtaining bone tissue engineering scaffolds. In particular, the nanofibrous structure is more similar to that of the natural bone extracellular matrix (ECM), and may bring additional stimulus to the cultured cells [26, 27].

Actually, the nanofibrous composite scaffolds have attracted much attention, and are readily prepared by mixing HA with synthetic or natural polymers such as PLA, poly(ε-caprolactone) (PCL), collagen, gelatin or chitosan [28–34]. PLGA (50/50 or 85/15)/HA fibrous composite scaffolds were also prepared, but they were mainly used for drug delivery instead of bone repair [4, 35, 36]. To our best knowledge, so far less concern has been paid to the PLGA/HA electrospun nanofibrous composite scaffolds in terms of bone regeneration and comprehensive assessments of the physical and biological properties. It must be pointed out that the biological properties of this class of fibrous composites depend on many factors including the origin of polymer matrix, HA particles and the fabrication conditions. In this work, hydroxyapatite nanoparticles (HAp) are incorporated into the PLGA fiber matrix by electrospinning the suspension of HAp/PLGA. Biological assessment is further performed in terms of cell proliferation and phenotype preservation. Thus the use of this composite nanofibrous scaffolds for bone repair shall be assessed, forwarding a new step to its potential applications in tissue engineering.

2 Materials and methods

2.1 Materials

Poly(lactide-co-glycolide) (PLGA, LA/GA 85/15, M_w = 200 kDa) was purchased from China Textile Academy. Tetrahydrofuran (THF) was purchased from Hangzhou Shuanglin Chemical Company, China. *N*,*N*-dimethyl formamide (DMF) and ethylenediamine tetraacetic acid disodium salt (EDTA) were bought from Sinopharm Chemical Reagent Co., Ltd. *p*-Nitrophenyl phosphate (*p*NPP) and tris(hydroxymethyl)aminomethane (Tris) were obtained from Shanghai qcbio Science & Technologies Co., Ltd. and Shanghai Sangon Biological Engineering Technology & Service Co., Ltd., respectively. Dulbecco's minimum essential medium (DMEM) and sodium dodecyl sulfonate (SDS) were purchased from Sigma-Aldrich. All other chemicals and bioreagents were used as received.

2.2 Preparation of hydroxyapatite particles

The hydroxyapatite particles (HAp) were prepared by chemical coprecipitation through aqueous solution [23, 37]. Briefly, 100 ml 0.1 M $(NH_4)_2HPO_4$ solution containing 50 g/l poly(ethylene glycol) (PEG) was dropped into 60 ml 0.1 M $CaCl_2$ solution (containing 50 g/l PEG) at a final Ca/P molar ratio of 1.67. The system was maintained at 4°C and pH 10 under agitation for 30 min. After extensively washed by triple-distilled water, the precipitates were frozen at −20°C for 2 h and lyophilized for another 48 h. The hydroxyapatite powders were obtained after calcining the dried precipitates at 900°C for 4 h and followed by sonication in ethanol for 20 min. The size of the HAp was determined in ethanol suspension at 25°C by dynamic light scattering (DLS, Brookhaven 90 plus) with five parallel specimens.

2.3 Electrospinning of PLGA/HAp nanofibrous composite scaffolds

Pre-determined amount of the HAp powders was added into 10 ml THF/DMF (1/1 volume ratio). The mixture was sonicated for 15 min to disperse the hydroxyapatite, into which 1.5 g PLGA was added and dissolved at 40°C overnight. The mixture was further magnetically stirred for 15 min, followed by ultrasonication for another 15 min to obtain the well-mixed PLGA/HAp suspension with a PLGA concentration of 15 wt%.

The PLGA/HAp nanofibrous composite scaffold was prepared by electrospinning of the mixture suspension. Briefly, the as-prepared suspension was added into a plastic syringe equipped with a needle with an inner diameter of 1.2 mm. The syringe was then mounted onto a syringe

pump (Medical Instrument Co., Ltd. of Zhejiang University, China), in which the needle was connected to a high-voltage power supply (Dongwen High Voltage Power Supply, China). Under 12 kV voltage, the fluid jet was injected out at a rate of 1.0 ml/h and the resultant nanofibers were collected on an aluminum foil which was put at 15 cm distance down from the needle. After electrospinning for 2 h at room temperature, the PLGA/HAp nanofibrous composite scaffold was obtained. Pure PLGA nanofibers were also prepared as the control. The nanofibrous scaffolds were dried in ventilating cabinet for 24 h to evaporate the residual solvent.

3 Characterizations

3.1 Morphology observation

After coated with a thin gold layer, the HAp and scaffolds were observed under a scanning electron microscope (SEM, FEI SIRION-100). The affiliated energy-dispersive X-ray spectroscopy (EDS) was used to analyze the elements of the HAp. The diameter and pore size of the nanofibers were measured by an image analysis software (Image J) from at least 30 fibers. For transmission electron microscopy (TEM, JEM-200 CX) observation, the electrospun nanofibers were collected on a carbon-coated copper grid for 10 s, whereas the HAp suspension was dropped onto a carbon coated grid and dried at 37°C.

3.2 XRD characterization

The X-ray diffractometer (XRD, Thermo ARL XTRA) was used to determine the phase structure of the HAp, PLGA and PLGA/HAp nanofibrous scaffolds. XRD patterns were obtained in a 2θ angle ranging from 10°–60° at a scanning speed of 2°/min.

3.3 In vitro biomineralization property

The biomineralization property of the nanofibrous scaffolds was assessed by immersing the scaffolds in a simulated body fluid (SBF) [38, 39]. Briefly, the PLGA nanofibrous scaffolds with and without HAp were cut into rectangular pieces of 10 × 40 mm, and then incubated in 25 ml of a five-time-concentrated SBF (5 × SBF, 726.0 mM Na^+, 25.0 mM K^+, 7.5 mM Mg^{2+}, 12.5 mM Ca^{2+}, 760.0 mM Cl^-, 21.0 mM HCO_3^-, 5.0 mM HPO_4^{2-}, and 2.5 mM SO_4^{2-}, buffered at pH 6.8 with Tris and 1 M HCl) at 37°C for up to 14 days. Herein, the concentration of the SBF was improved to five times (5 × SBF) in order to accelerate the mineralization process for more apparent effect [38]. The fluid was changed every 2 days. After a period of time, the samples were taken out, thoroughly rinsed by distilled water to remove the adsorbed salts and then freeze-dried for 12 h. Morphology of the deposited apatite on the fiber surface was observed by SEM.

4 In vitro osteoblasts culture

4.1 Osteoblasts seeding

Neonatal mouse calvaria-derived MC3T3-E1 osteoblasts were a gift from Oral Medical Center, The First Affiliated Hospital of Zhejiang University. The cells were cultured in a 9 cm plastic tissue culture dish (Falcon) containing DMEM supplemented with 10% fetal bovine serum (FBS), 100 U/ml penicillin and 100 U/ml streptomycin. The medium was replaced every 2 days and the culture was maintained in a humidified atmosphere of 95% air and 5% CO_2 at 37°C. After the cells reached 80–90% confluence, they were detached using 0.25% trypsin in PBS and were resuspended in the supplemented culture medium, and used for the experiments.

The control PLGA and PLGA/HAp electrospun nanofibers were cut into circular pieces with a diameter of 7 mm, which could fully cover the bottom of a well of a 96-well tissue culture polystyrene plate (TCPS). Before cell seeding, the scaffolds were sterilized by 75% ethanol solution and UV irradiation of low power (the UV light in the biosafety cabinet) overnight. They were then washed by PBS (pH 7.4) before placed onto the culture well. Into each well 200 μl osteoblast suspension was seeded at a final density of 4×10^4 cells/well ($\sim 10.4 \times 10^4$ cells/cm^2). The cells were cultured statically in the DMEM culture medium under the conditions as described above.

4.2 Cell viability

The cell viability was measured by a MTT (3-(4,5-dimethyl) thiazol-2-yl-2,5-dimethyl tetrazolium bromide) assay. At a given culture time, 20 μl 5 mg/ml MTT solution was added into each well and the cells/scaffold constructs were continually cultured for another 4 h. During this period, viable cells could reduce the MTT to formazan pigment. After the cells/scaffold constructs were transferred to other wells, 200 μl dimethyl sulphoxide (DMSO) was added into each well to dissolve the formazan pigment. 150 μl of the DMSO solution was finally added into a well of another 96-well tissue culture plate, whose absorbance at 570 nm was recorded by a microplate reader (Bio-Rad 550). All data were averaged from three parallel experiments.

4.3 Cell attachment and proliferation

To determine the cell growth on the scaffolds, the cell number was assessed by quantifying DNA content in the constructs using Hoechst 33258 dye (Sigma) assay [40, 41]. The cells/scaffold constructs were taken out, washed with PBS twice and alternatingly freeze-thawed at −20°C for 3 times, each for 20 min. Each sample was then digested with 100 µl cell lysis buffer (0.8% (w/v) SDS, 100 mM Tris, 20 mM EDTA, pH 8.0) at 4°C for 12 h, followed by ultrasonication for another 15 min. Shortly after 60 µl of the digested solution was added into 2 ml Hoechst 33258 solution (1 µg/ml), the fluorescence intensity at 490 nm was measured by a luminescence spectrophotometer (LS 55, Perkin-Elmer) at an excitation wavelength of 360 nm. The cell number on the scaffolds was determined by referring to a calibration curve recorded from known number of osteoblasts at the same wavelength. All data were averaged from three parallel experiments.

4.4 Cell distribution and morphology

The distribution and morphology of the osteoblasts on the scaffolds was observed under SEM (Stereoscan 260, Cambridge) after the cells were cultured for 7 days. The cells/scaffold constructs were taken out from the culture plate and rinsed gently with PBS. After fixed by glutaraldehyde at 4°C for 24 h, they were dehydrated in graded ethanol solutions (30, 50, 75, 95 and 100%) and sequentially treated by isoamylacetate, each for 15 min at room temperature. Finally, observation was performed after critical point drying and gold coating.

4.5 Alkaline phosphatase (ALP) assay

ALP secretion of the osteoblasts cultured on the scaffolds was determined quantitatively using *p*-nitrophenyl phosphate (*p*NPP) solution as the reaction substrate [31]. Digestion of the cells/scaffold constructs was carried out as described above after removal from the culture wells. 100 µl lysed solution was incubated in 500 µl fresh *p*NPP-diethanolamine (DEA) solution (3 mM *p*NPP aqueous solution mixed in equivalent volume of 20% (v/v) DEA solution containing 10 mM $MgCl_2{\cdot}6H_2O$ and 3.9% (v/v) 12 M HCl) at a 37°C water bath for 30 min. 500 µl 0.1 M aqueous NaOH solution was successively added to terminate the reaction. The product of *p*-nitrophenyl (*p*NP, the enzymatic product of *p*NPP) in the presence of ALP was immediately measured at 405 nm on a UV–vis spectrophotometer (UV-Probe 2550, Shimadzu). A calibration curve was obtained with aqueous *p*-nitrophenyl solution recorded at the same conditions. The calculation is based on the assumption that 1 mol ALP hydrolyzes exactly 1 mol *p*NPP substrate. All data were averaged from three parallel experiments.

4.6 Statistical analysis

Data are expressed as mean ± standard deviation (SD). Statistical analysis was performed by two-population Student's *t*-test. The significant level was set as $P < 0.05$.

5 Results and discussion

5.1 Characterization of HA nanoparticles

It has been well demonstrated that the nano-HA particles not only possess good bioactivity and osteoconductivity, but can also improve the mechanical strength of the scaffolds [1, 2]. Apart from animal natural bone source, the nano-HA particles can be prepared by a variety of approaches, for example, the wet chemical/precipitation [2] which was employed in this work. The stabilizer PEG molecules [37] were removed after high temperature calcining. Figure 1a shows that the initially calcined HAp aggregated into irregular granules, which could be dispersed into a smaller size with narrower distribution after ultrasonication (Fig. 1b). The particles had a spherical shape (Fig. 1c) with a uniform average size of 266.6 ± 7.3 nm measured by DLS. The phenomenon of necking among the particles should be caused by localized sintering [42]. EDS confirmed that the major elements of the HAp were calcium (Ca) and phosphorus (P) with an atomic ratio of 1.634 (Fig. 1d), which is close to the theoretical value of 1.67 for HAp (stoichiometric formula $Ca_{10}(PO_4)_6(OH)_2$) [2]. XRD pattern also revealed the pure hydroxyapatite phase with high crystallinity (Fig. 4c) according to JCPDS Card 9-432. The particle size is one of the crucial factors influencing the integrity of the scaffolds, especially for the nanofibrous scaffolds when the HAp are incorporated into the polymer matrix [9, 10]. Since the diameter of the electrospun PLGA fibers was in a submicro scale as reported in our previous study [43], incorporation of the as-prepared HAp into the PLGA matrix by co-electrospinning can be then processed.

5.2 Morphology and structure of the nanofibrous scaffolds

In composite materials, the surface and inner structure and distribution of the components have a decisive impact on the materials properties. For tissue engineering application, distribution of the HAp in-and-outside the fibers will further influence cytocompatibility of the scaffolds, such as cell adhesion and proliferation. Therefore, morphology and

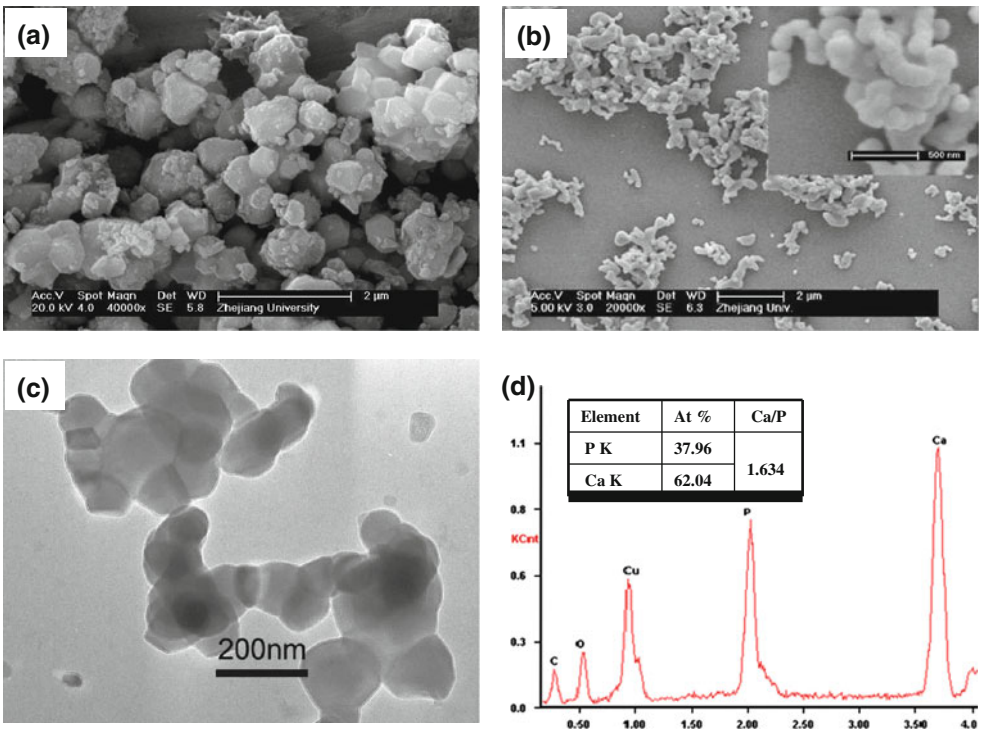

Fig. 1 **a** and **b** SEM images of the calcined hydroxyapatite particles (HAp) before (**a**) and after (**b**) ultrasonication. **c** and **d** are TEM image and energy-dispersive X-ray spectrum (EDS) of the HAp after ultrasonication, respectively

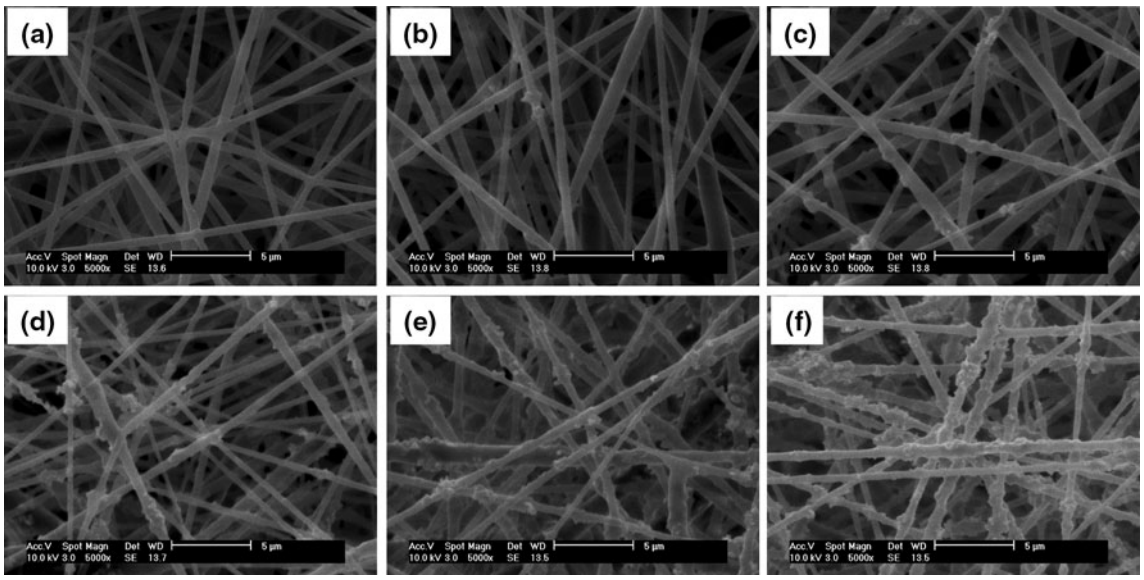

Fig. 2 SEM images to show surface morphology of: **a** PLGA, **b** PLGA/0.5HAp, **c** PLGA/2.5HAp, **d** PLGA/5HAp, **e** PLGA/10HAp, and **f** PLGA/15HAp nanofibrous scaffolds

structure of the pure PLGA and PLGA/HAp electrospun scaffolds were observed under SEM and TEM, as shown in Figs. 2 and 3. In this experiment, a series of PLGA/HAp composite nanofibers with different HAp amount were fabricated. For convenience of expression, the symbol of % was omitted, for example, addition of 1 and 10 wt% HAp was designated as 1HAp and 10HAp, respectively.

Both the control PLGA and PLGA/HAp electrospun scaffolds showed a randomly interconnected and highly porous structure which was composed of continuous

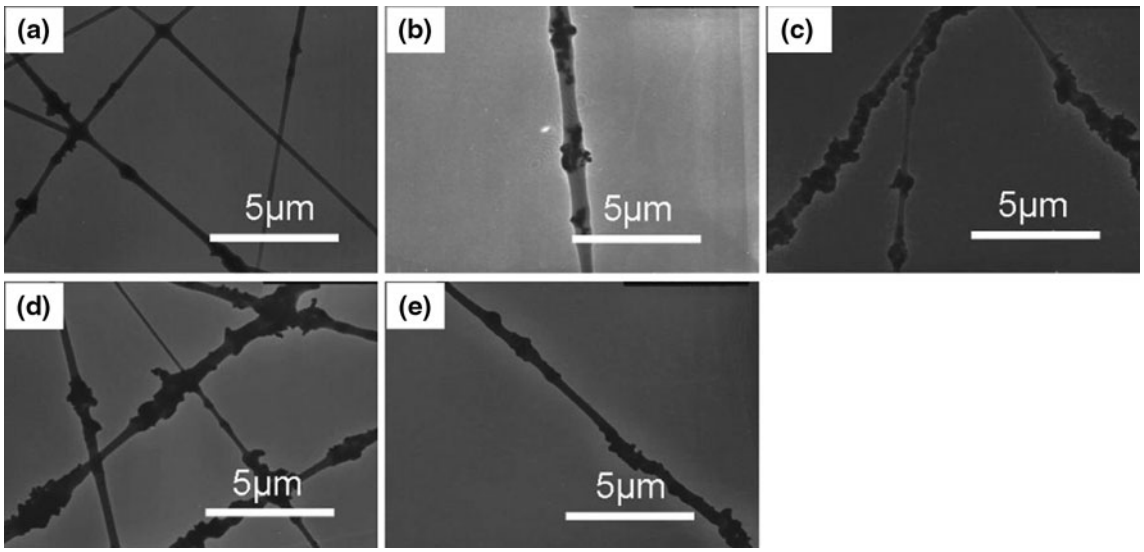

Fig. 3 TEM images to show inner structure of nanofibrous scaffolds. **a** PLGA/0.5HAp, **b** PLGA/2.5HAp, **c** PLGA/5HAp, **d** PLGA/10HAp and **e** PLGA/15HAp

Table 1 Diameter and pore size of nanofibrous scaffolds

Sample	Diameter (nm)	Pore size (nm)
PLGA	421 ± 117	3802 ± 1163
PLGA/0.5HAp	494 ± 117	3071 ± 998
PLGA/2.5HAp	587 ± 229	4443 ± 1222
PLGA/5HAp	556 ± 317	3573 ± 921
PLGA/10HAp	569 ± 213	4317 ± 1280
PLGA/15HAp	537 ± 108	4206 ± 917

bead-free nonwoven nanofibers (Fig. 2). The fiber diameter increased from 421 ± 117 nm (for the PLGA) to 494 ± 117 nm and further to 550–590 nm after addition of 0.5HAp and higher amount of HAp, respectively (Table 1). This size just falls in the range of collagen fibers of bone (100–2000 nm) [2], which enables the scaffolds with a structural similarity. However, the pore size of all the scaffolds remained more or less constant with an average value of ~4000 nm regardless of the HAp addition. This is quite common for the electrospun fibrous scaffolds, in which the pores are formed by the alignment of the injected fibers and thereby can be only varied within a small range. This is consistent with a previous study, in which the pore size was not significantly varied although the diameter of polystyrene nanofibers was decreased along with the increase of voltage [44].

However, surface structure of the nanofibers varied apparently after addition of the HAp. Compared with a smooth morphology of the control PLGA nanofibers (Fig. 2a), rough surfaces were observed for all the composite scaffolds (Fig. 2b–f). A few tiny particles were found on the fiber surfaces when 0.5HAp was added (Fig. 2b). Addition of 2.5HAp resulted in a structure with some nanoparticle protuberances on the fiber surfaces (Fig. 2c), whereas 5HAp and 10HAp yielded larger agglomerates uniformly distributing on the fiber surfaces (Fig. 2d, e). When the amount was further increased to 15HAp, the surface of the fibers was even entirely covered by a layer of nanoparticles (Fig. 2f). Similar phenomenon was also observed by Thomas et al. [32], in which surface roughness of collagen/20% nanoHA composite fibers was substantially larger than that of pure collagen fibers. Deng et al. [28] also reported the coarseness of the PLLA/HA hybrid nanofibrous scaffolds, although the average fiber diameter did not vary significantly. In this regard, the electrospun composite nanofibers of PLGA and HA could better mimick the micro/nano-structure of the natural bone [2].

TEM images revealed the inner structure of the nanofibers more clearly. When the content of HAp was lower than 2.5 (Fig. 3a, b), the particles resided mainly inside the fibers with slight agglomeration. With increase of the HAp amount, the agglomeration became serious, and more and more particles attached on the fiber surfaces (Fig. 3c–e). This observation is in good accordance with the SEM micrographs (Fig. 2) and consistent with the structure of the HAp (Fig. 1), revealing the successful fabrication of the bone structure biomimetic PLGA/HAp nanofibrous composite scaffolds.

5.3 X-ray diffraction of the nanofibrous scaffolds

In order to study the crystalline structure of the HAp in the nanocomposite, XRD characterization was performed (Fig. 4). Appearance of the broad peaks in the $2\theta =$ 10°–25° region was attributed to the amorphous nature of

the PLGA copolymer (Fig. 4a, b). After incorporation of HAp, the patterns of the composite scaffolds (here taking the PLGA/2.5HAp nanofibers as a typical example) exhibited several peaks at $2\theta = 25.9°$, 27.8°, 29.0°, 31.8°, 32.2°, 32.9°, 34.3°, 39.8° and 46.7° which correspond to (002), (102), (210), (211), (112), (300), (202), (310) and (222) typical spectrum of HAp (Fig. 4c), respectively [45]. Together with the structure observation and FTIR spectra (Fig. S1 of the Supporting Information), one can conclude that the crystalline structure of the HAp had been preserved in the nanofibrous composite scaffolds.

5.4 In vitro biomineralization ability of the nanofibrous scaffolds

Biomineralization ability of biomaterials is one of the important properties governing their application in bone regeneration. The mineralization occurred in a five-time-concentrated SBF (5 × SBF) to different extents as shown in Fig. 5. The first column of Fig. 5 shows that no notable bone-like apatite was formed on the PLGA nanofibers (Fig. 5a1) after incubated for 1 day, but some bone-like apatite minerals were observed on the composite scaffolds (representative by the PLGA/5HAp nanofibers) (Fig. 5b1) in comparison with their initial morphology (Fig. 2). Higher magnification of the minerals revealed that they were composed of flake crystals (Fig. 5b1h). Along with prolongation of the incubation time, the mineralization was hardly enhanced on the PLGA nanofibers, but more mineral microparticles were deposited on the PLGA/5HAp nanofibers, in which bead-like structure was formed along the nanofibers (Fig. 5b2) after 4 days and further developed into necklace after 14 days (Fig. 5b3). Similar increase of the bone-like minerals was observed by Schneider et al. [46] and Zhang et al. [47] after PLGA/amorphous tricalcium phosphate (ATCP) electrospun nanocomposites were immersed in SBF and the electrospun PLGA (75/25)/multi-walled carbon nanotubes (MWNTs) nanofibers were incubated into 1.5 × SBF solutions up to 21 days, respectively. Therefore, this result confirms that the PLGA alone have little ability to induce the bone-like mineral growth due to its hydrophobic nature and lack of sufficient functional groups, while the incorporated HAp particles could function as nucleation sites to accelerate the mineral growth [48]. During formation of the natural bone, the hydroxyapatite crystals are gradually bound to the collagen fibers via a self-assembly mineralization mode [49]. While the composition of SBF was close to that of the blood plasma [38], the result of stronger biomineralization ability of the PLGA/HAp nanofibers may indicate that they have a better bioactivity to induce calcium mineralization for bone regeneration. Actually, it was reported that PLGA/HA 3D composite scaffolds exhibited better performance in mineral deposition and osteogenesis either cultured with osteoblasts in vitro [50] or embedded in rabbit dorsal muscles in vivo [20].

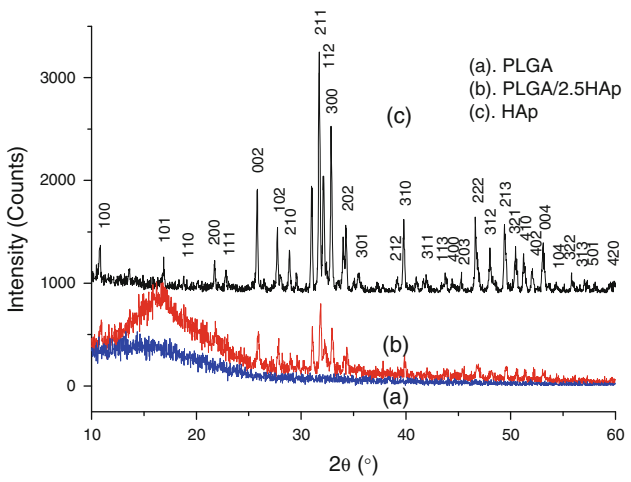

Fig. 4 X-ray diffraction patterns of: **a** PLGA, **b** a representative nanofibrous scaffold of PLGA/2.5HAp and **c** HAp

Considering the structure (Figs. 2, 3), mechanical properties (Fig. S2 of the Supporting Information) and degradability (Fig. S3 of the Supporting Information) of the PLGA nanofibrous scaffolds with different amount of HAp, the PLGA/5HAp nanofibrous scaffold with much uniform distribution of HAp were chosen as a representative for the next study, so that the sample number could be maximally reduced while the common effects of the incorporated HAp could be universally disclosed. Comparison was made by using pure PLGA scaffold as a control to evaluate the in vitro cell viability, proliferation, morphology, and ALP activity as shown in Figs. 6, 7, 8.

5.5 Viability and proliferation of osteoblasts

The cell viability on all the samples showed almost same alteration tendency along with prolongation of the culture time (Fig. 6a), namely increased very sharply along with the culture time until day 7 ($P < 0.05$), and then decreased slowly until day 14. No significant difference was found between the control PLGA and PLGA/5HAp nanocomposites at each time interval ($P > 0.05$).

Figure 6b shows attachment and proliferation of the osteoblasts on the control PLGA and PLGA/5HAp nanofibrous scaffolds. The initially seeded 10.4×10^4 cells/cm^2 resulted in approximately 2.3×10^4 cells/cm^2 attachment on the PLGA/5HAp nanofibrous scaffolds after 24 h culture, namely only 22.5% attachment percentage, which was comparable with those on the control PLGA scaffolds ($P > 0.05$). This value is close to that (~24.0%) of NIH-3T3 fibroblasts cultured on poly(L-lactide-co-caprolactone) (PLCL) (50/50) and PLCL/gelatin blended fibers [51] and

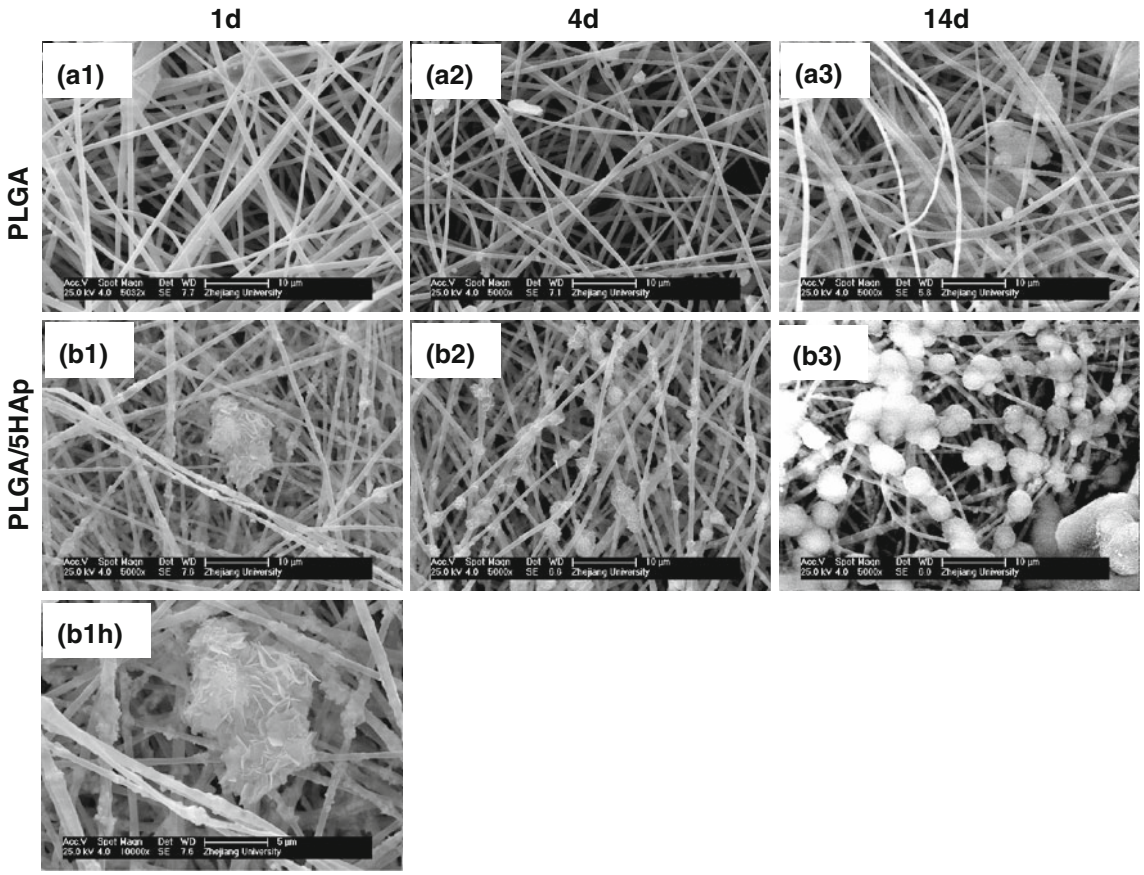

Fig. 5 SEM images of: **a** control PLGA and **b** PLGA/5HAp scaffolds mineralized in 5 × SBF at 37°C for 1−14 days, respectively. (**b1h**) is higher magnification of (**b1**)

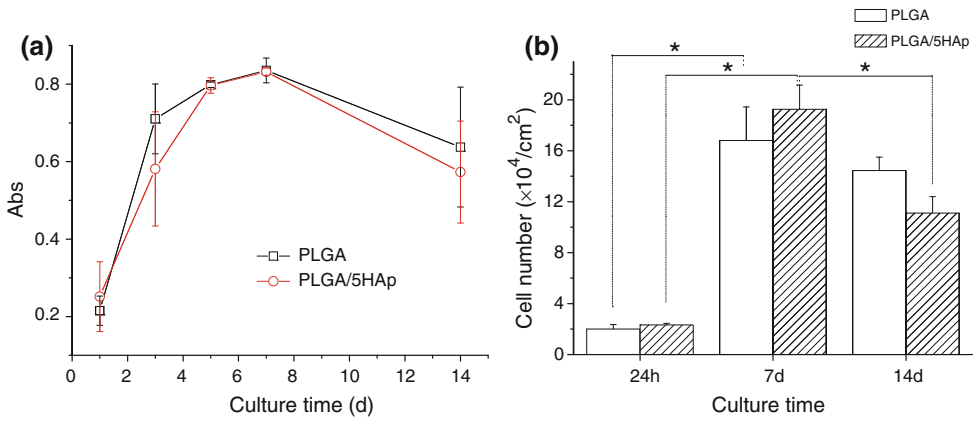

Fig. 6 **a** Viability and **b** proliferation of MC3T3-E1 osteoblasts on the control PLGA and PLGA/5HAp nanofibrous scaffolds as a function of culture time. $^*P < 0.05$

that (∼22.8%) of chondrocytes cultured on 50% PLGA (85/15) microspheres integrated gelatin/chitosan/hyaluronan scaffolds [52]. However, it is substantially smaller than that (∼66.5%) of rat calvarial osteoblasts cultured in PLGA (75/25)/HA composite scaffolds fabricated by gas forming and particulate leaching (GF/PL) [50] and that (∼72.2%) of mouse calvaria-derived pre-osteoblasts (MC3T3-E1) cultured on electrospun PCL/HAp fiber mats [31]. The discrepancies might be caused by the differences in cell types, culture mediums and methods for injecting

cells onto the scaffolds. In our case, observation showed that some of the cells leaked from the scaffolds and attached on the TCPS surface.

After 7 days culture, the cell number on both types of the specimens was improved by a factor of ~ 10 ($P < 0.05$), indicating that the fibrous scaffolds were able to support cell proliferation. Slightly larger average number of cells were counted on the HAp-embedded PLGA scaffolds, but the difference was not significant ($P > 0.05$). When the culture time was prolonged to 14 days, the cell proliferation was decayed on both types of the scaffolds compared with day 7 ($P < 0.05$), but no significant difference was found between these two specimens ($P > 0.05$). This is in a good accordance with the cell viability (Fig. 6a), showing that the HAp incorporation did not bring strong influence on osteoblast proliferation. Similarly, Ngiam's study [48] demonstrated that the osteoblast number on mineralized PLGA (75/25) nanofibers was even smaller than that on the pure PLGA nanofibers after day 4 and 7. Likewise, Wutticharoenmongkol et al. [31] reported the cell number on PCL/HAp fiber mats was comparable to that on PCL fiber mats during the first 2 days cell culture, and just slightly greater than the latter until 3 days. Nevertheless, proliferation of osteoblasts was improved significantly on electrospun hydroxyapatite/chitosan scaffolds [34] and nano-HA/collagen/poly(lactic acid) (nHAC/PLA) scaffolds [53]. This may imply that the HAp crystal itself has little influence on cell adhesion and proliferation, but the material properties such as surface chemistry, topography and energy may likely work [48]. For instance, the ultrathin nanofibers themselves might have already played important roles in stimulating cell growth by forming focal contacts [26, 27]. Evidence also shows that the attachment of cells (e.g., osteoblasts, fibroblasts and human mesenchymal stem cells (hMSCs)) was affected by material chemistry and grain size instead of surface roughness and crystal phase [54]. Moreover, considering that the ratio between the viability at day 7 to day 1 was only ~ 3 (Fig. 6), one can conclude that the general metabolic activity of the cells does not simultaneously improve as that of their proliferation. The cell number decrease at 14 days is known to be caused by the contact inhibition effect when the cell number becomes pretty large.

5.6 Cell distribution and morphology

The morphology of the cells attached on these nanofibrous scaffolds was subject to SEM investigation after culture for 7 days (Fig. 7). No apparent changes were found for all the scaffolds in terms of the randomly interconnected porous structure regardless of UV irradiation and cell culture. The cells on the PLGA/5HAp scaffolds seemed more spreading, i.e., each cell covered a relatively larger area with a lot of nanofibers (Fig. 7b) than that on the control PLGA fibrous scaffolds (Fig. 7a). A higher magnification showed that the cells on the PLGA/5HAp scaffolds connected with each other by their pseudopodia. The SEM images reveal also there were slightly more osteoblasts on the PLGA/5HAp nanofibrous scaffolds (Fig. 7b), which is basically consistent with the quantitative average cell numbers shown in Fig. 6b. This is consistent with a previous study, which showed that incorporation of L-lactic acid oligomer surface grafted HA particles into PLGA porous composite scaffolds can enhance osteoblast proliferation and spreading areas compared with the pure PLGA scaffolds [55].

5.7 ALP activity

ALP is an enzyme secreted by osteoblasts and acts as one of the markers to confirm the osteoblastic phenotype and mineralization [31, 56]. To further testify the cell functions on the nanofibrous scaffolds, the ALP activity was measured at days 5, 7 and 14 as shown in Fig. 8. The osteoblasts on both types of scaffolds could normally secrete ALP after cultured for 5 days. However, only the activity of ALP secreted by the cells on the PLGA/5HAp specimens increased along with the culture time, and reached a maximum level at 7 days and then slightly decreased after 14 days. In contrast, the ALP activity of the cells grown on the control PLGA scaffolds showed a slight decrease tendency during the culture time. While no significant difference was detected at a culture time of 5 days among the samples ($P > 0.05$), significant difference was indeed found between the PLGA/5HAp and control PLGA scaffolds after 7 and 14 days culture ($P < 0.05$). For instance, the ALP activity was quantified to be 9.6 nmol/cm^2 on the PLGA/5HAp nanofibers at 7 days, which was 60.0% higher than that on the control PLGA nanofibers (5.9 nmol/cm^2). This is consistent with the previous studies by using other types of HA-containing composite scaffolds or nanofibers [48]. The nano-HA particles are likely able to bind the serum proteins and growth factors and thereby improve cell metabolic activities and maintain cell phenotype [57]. Furthermore, the ALP synthesis by the osteoblasts was reported to be affected by both the cell numbers and bone-like minerals which act as nuclei of calcification [31, 56]. The comparable cell number on the both types of scaffolds (Fig. 6b) would imply that each cell on the PLGA/5HAp scaffold secretes more ALP and thereby has better performance in phenotype preservation, which is in good accordance with the in vitro biomineralization (Fig. 5). Taking into account the cell viability and proliferation, it could draw that the HAp took the key role on triggering osteoblastic phenotype expression, but less on supporting cell viability, adhesion and proliferation. Therefore, the PLGA nanofibers integrated with the HAp are more attractive to be used as a biomimetic scaffold for bone regeneration.

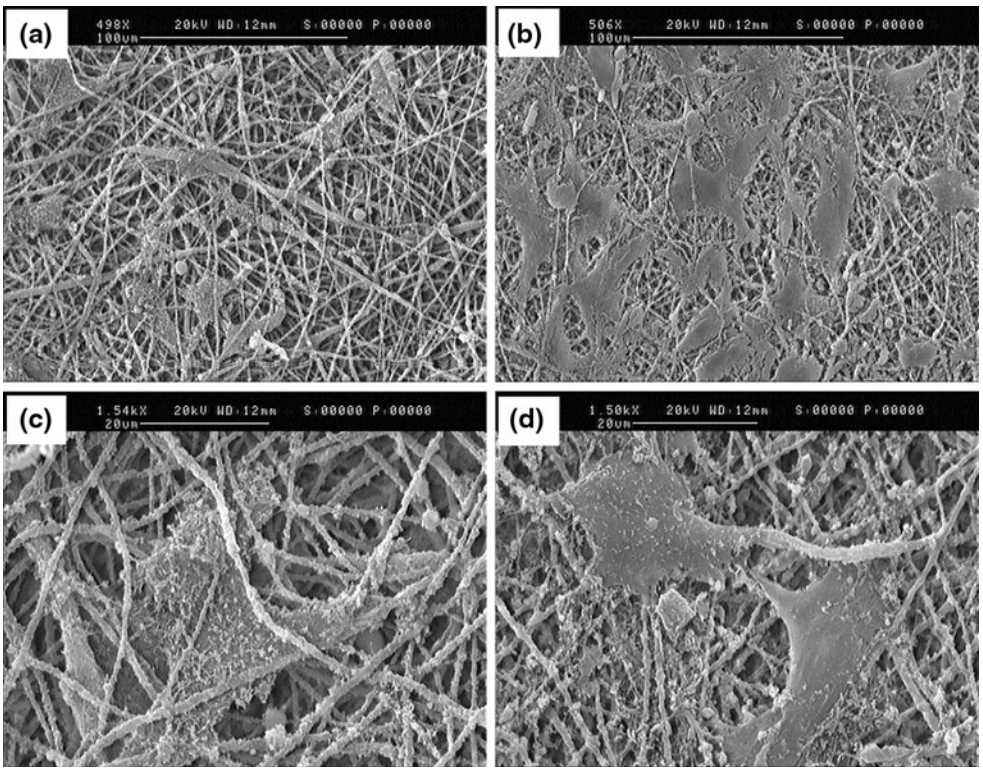

Fig. 7 SEM images to show cell morphology on: **a** the control PLGA and **b** PLGA/5HAp nanofibrous scaffolds after culture for 7 days. **c** and **d** are higher magnification of **a** and **b**, respectively. Cell seeding density was 4×10^4 cells/well (approximately 10.4×10^4 cells/cm^2)

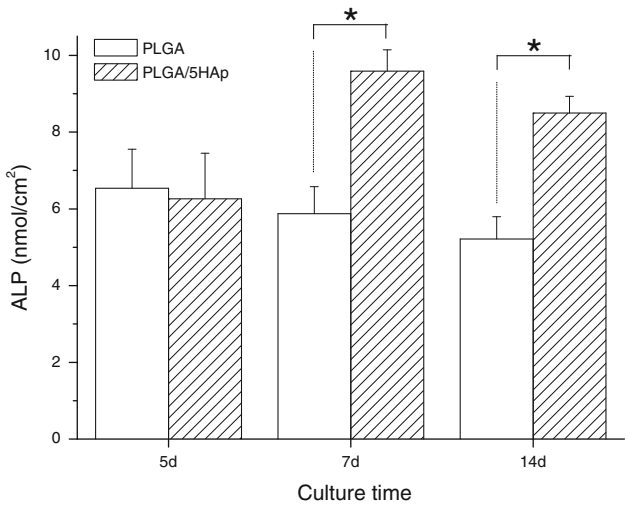

Fig. 8 ALP activity of MC3T3-E1 osteoblasts seeded on the control PLGA and PLGA/5HAp nanofibrous scaffolds after 5, 7 and 14 days culture. Cell seeding density was 4×10^4 cells/well (approximately 10.4×10^4 cells/cm^2). $^*P < 0.05$

The preliminary results render further investigation and applications. For example, a still longer term cell culture would be beneficial to clarify the bone formation ability especially by detecting osteogenic and biomineralization markers. Furthermore, by implanting the nanofibrous scaffolds into animal tissues such as the subcutaneous space of athymic mice or rabbit dorsal muscles, it will be more justified to evaluate the full potential of the nanofibrous scaffolds as candidates for bone regeneration.

6 Conclusions

Biodegradable PLGA nanofibrous composite scaffolds incorporated with bone matrix-mimic hydroxyapatite particles were successfully prepared by electrospinning of PLGA solution having the HAp. At a lower concentration, the HAp was uniformly dispersed on the fiber surfaces. Along with increase of the HAp concentration, larger agglomerates gradually covered on the fibers. Biomineralization in the PLGA/HAp nanofibrous scaffolds was pronouncedly enhanced than that in the control PLGA scaffolds. In vitro culture of MC3T3-E1 osteoblasts found that the cells could proliferate on both the samples with a sharp increase of viability until day 7, and then decreased to some extent until day 14. The cells cultured on the PLGA/5HAp scaffolds showed significantly higher ALP activity than that on the control PLGA scaffolds by a factor of 60.0% at 7 days. Therefore, integration of the HAp with the PLGA nanofibers is a meaningful way to obtain nanofibrous scaffolds with better physical and biological performance, which are more attractive for bone regeneration too.

Acknowledgments This study is financially supported by the Natural Science Foundation of China (20934003), and the Science and Technology Program of Zhejiang Province (2009C14003, 2009C13020).

References

1. Webster TJ, Ahn ES. Nanostructured biomaterials for tissue engineering bone. Adv Biochem Eng Biotechnol. 2007;103: 275–308.
2. Murugan R, Ramakrishna S. Development of nanocomposites for bone grafting. Compos Sci Technol. 2005;65:2385–406.
3. Boyle WJ, Simonet WS, Lacey DL. Osteoclast differentiation and activation. Nature. 2003;423:337–42.
4. Jose MV, Thomas V, Johnson KT, Dean DR, Nyalro E. Aligned PLGA/HA nanofibrous nanocomposite scaffolds for bone tissue engineering. Acta Biomater. 2009;5:305–15.
5. Sopyan I, Mel M, Ramesh S, Khalid KA. Porous hydroxyapatite for artificial bone applications. Sci Technol Adv Mater. 2007;8: 116–23.
6. Rose FRAJ, Oreffo ROC. Bone tissue engineering: hope vs hype. Biochem Biophys Res Commun. 2002;292:1–7.
7. Burg KJL, Porter S, Kellam JF. Biomaterial developments for bone tissue engineering. Biomaterials. 2000;21:2347–59.
8. Hutmacher DW. Scaffolds in tissue engineering bone and cartilage. Biomaterials. 2000;21:2529–43.
9. Huang ZM, Zhang YZ, Kotaki M, Ramakrishna S. A review on polymer nanofibers by electrospinning and their applications in nanocomposites. Compos Sci Technol. 2003;63:2223–53.
10. Sill TJ, von Recum HA. Electro spinning: applications in drug delivery and tissue engineering. Biomaterials. 2008;29:1989–2006.
11. Schreuder-Gibson H, Gibson P, Wadsworth L, Hemphill S, Vontorcik J. Effect of filter deformation on the filtration and air flow for elastomeric nonwoven media. Adv Filtr Sep Technol. 2002; 15:525–37.
12. Bergshoef MM, Vancso GJ. Transparent nanocomposites with ultrathin, electrospun nylon-4,6 fiber reinforcement. Adv Mater. 1999;11:1362–5.
13. Wang XY, Drew C, Lee SH, Senecal KJ, Kumar J, Sarnuelson LA. Electrospun nanofibrous membranes for highly sensitive optical sensors. Nano Lett. 2002;2:1273–5.
14. Jing Z, Xu XY, Chen XS, Liang QZ, Bian XC, Yang LX, Jing XB. Biodegradable electrospun fibers for drug delivery. J Control Release. 2003;92:227–31.
15. Liang D, Hsiao BS, Chu B. Functional electrospun nanofibrous scaffolds for biomedical applications. Adv Drug Deliver Rev. 2007;59:1392–412.
16. Chronakis IS. Novel nanocomposites and nanoceramics based on polymer nanofibers using electrospinning process—a review. J Mater Process Technol. 2005;167:283–93.
17. Lao LH, Tan HP, Wang YJ, Gao CY. Chitosan modified poly(L-lactide) microspheres as cell microcarriers for cartilage tissue engineering. Colloid Surf B. 2008;66:218–25.
18. Tan HP, Wan L, Wu JD, Gao CY. Microscale control over collagen gradient on poly(L-lactide) membrane surface for manipulating chondrocyte distribution. Colloid Surf B. 2008;67:210–5.
19. Seal BL, Otero TC, Panitch A. Polymeric biomaterials for tissue or organ regeneration. Mater Sci Eng. 2001;34:147–230.
20. Zhang PB, Hong ZK, Yu T, Chen XS, Jing XB. In vivo mineralization and osteogenesis of nanocomposite scaffold of poly (lactide-co-glycolide) and hydroxyapatite surface-grafted with poly(L-lactide). Biomaterials. 2009;30:58–70.
21. Nelson JF, Stanford HG, Cutright DE. Evaluation and comparison of biodegradable substances as osteogenic agents. Oral Surg. 1977;43:836–43.
22. Hollinger JO. Preliminary report on the osteogenic potential of a biodegradable copolymer of polyactide (PLA) and polyglycolide (PGA). J Biomed Mater Res. 1983;17:71–82.
23. Zhao HG, Ma L, Gao CY, Wang JF, Shen JC. Fabrication and properties of injectable beta-tricalcium phosphate particles/fibrin gel composite scaffolds for bone tissue engineering. Mater Sci Eng C. 2009;29:836–42.
24. Gay S, Arostegui S, Lemaitre J. Preparation and characterization of dense nanohydroxyapatite/PLLA composites. Mater Sci Eng C. 2009;29:172–7.
25. Rizzi SC, Heath DT, Coombes AGA, Bock N, Textor M, Downes S. Biodegradable polymer/hydroxyapatite composites: surface analysis and initial attachment of human osteoblasts. J Biomed Mater Res. 2001;55:475–86.
26. Woo KM, Jun JH, Chen VJ, Seo J, Baek JH, Ryoo HM, Kim GS. Nano-fibrous scaffolding promotes osteoblast differentiation and biomineralization. Biomaterials. 2007;28:335–43.
27. Martinez E, Engel E, Planell JA, Samitier J. Effects of artificial micro- and nano-structured surfaces on cell behaviour. Ann Anat. 2009;191:126–35.
28. Deng XL, Sui G, Zhao ML, Chen GQ, Yang XP. Poly(L-lactic acid)/hydroxyapatite hybrid nanofibrous scaffolds prepared by electrospinning. J Biomater Sci Polym Ed. 2007;18(1):117–30.
29. Sui G, Yang X, Mei F, Hu X, Chen G, Deng X, Ryu S. Poly-L-lactic acid/hydroxyapatite hybrid membrane for bone tissue regeneration. J Biomed Mater Res A. 2007;82(2):445–54.
30. Kim HW, Lee HH, Knowles JC. Electrospinning biomedical nanocomposite fibers of hydroxyapaite/poly(lactic acid) for bone regeneration. J Biomed Mater Res A. 2006;79A:643–9.
31. Wutticharoenmongkol P, Pavasant P, Supaphol P. Osteoblastic phenotype expression of MC3T3–E1 cultured on electrospun polycaprolactone fiber mats filled with hydroxyapatite nanoparticles. Biomacromolecules. 2007;8:2602–10.
32. Thomas V, Dean DR, Jose MV, Mathew B, Chowdhury S, Vohra YK. Nanostructured biocomposite scaffolds based on collagen coelectrospun with nanohydroxyapatite. Biomacromolecules. 2007;8:631–7.
33. Kim HW, Song JH, Kim HE. Nanofiber generation of gelatin/hydroxyapatite biomimetics for guided tissue regeneration. Adv Funct Mater. 2005;15:1988–94.
34. Zhang Y, Venugopal JR, El-Turki A, Ramakrishna S, Su B, Lim CT. Electrospun biomimetic nanocomposite nanofibers of hydroxyapatite/chitosan for bone tissue engineering. Biomaterials. 2008;29:4314–22.
35. Nie HM, Wang CH. Fabrication and characterization of PLGA/HAp scaffolds for delivery of BMP-2 plasmid composite DNA. J Control Release. 2007;120:111–21.
36. Nie H, Soh BW, Fu YC, Wang CH. Three-dimensional fibrous PLGA/HAp composite scaffold for BMP-2 delivery. Biotechnol Bioeng. 2008;99:223–34.
37. Li YB, Weng WJ, Cheng K, Du PY, Shen G, Wang JX, Han GR. Preparation of amorphous calcium phosphate in the presence of poly(ethylene glycol). J Mater Sci Lett. 2003;22:1015–6.
38. Jayasuriya AC, Shah C, Ebraheim NA, Jayatissa AH. Acceleration of biomimetic mineralization to apply in bone regeneration. Biomed Mater. 2008;3:015003.
39. Kim SS, Park MS, Gwak SJ, Choi CY, Kim BS. Accelerated bonelike apatite growth on porous polymer/ceramic composite scaffolds in vitro. Tissue Eng. 2006;12:2997–3006.
40. Kim YJ, Sah RLY, Doong JYH, Grodzinsky AJ. Fluorometric assay of DNA in cartilage explants using Hoechst-33258. Anal Biochem. 1988;174:168–76.

41. Ameer GA, Mahmood TA, Langer R. A biodegradable composite scaffold for cell transplantation. J Orthop Res. 2002;20:16–9.
42. Kwon SH, Jun YK, Hong SH, Kim HE. Synthesis and dissolution behavior of β-TCP and HA/β-TCP composite powders. J Eur Ceram Soc. 2003;23:1039–45.
43. Wang YJ, Gao CY. Influence of solvent volatility on diameter and dynamical mechanical strength of electrospun PLGA fibers. J Tissue Eng Reconstr Surg. 2007;3:7–10.
44. Megelski S, Stephens JS, Chase DB, Rabolt JF. Micro- and nanostructured surface morphology on electrospun polymer fibers. Macromolecules. 2002;35:8456–66.
45. Silva CC, Pinheiro AG, Miranda MAR, Goes JC, Sombra ASB. Structural properties of hydroxyapatite obtained by mechanosynthesis. Solid State Sci. 2003;5:553–8.
46. Schneider OD, Loher S, Brunner TJ, Uebersax L, Simonet M, Grass RN, Merkle HP, Stark WJ. Cotton wool-like nanocomposite biomaterials prepared by electrospinning: in vitro bioactivity and osteogenic differentiation of human mesenchymal stem cells. J Biomed Mater Res B. 2008;84(2):350–62.
47. Zhang HL, Liu JS, Yao ZW, Yang J, Pan LZ, Chen ZQ. Biomimetic mineralization of electrospun poly (lactic-co-glycolic acid)/multi-walled carbon nanotubes composite scaffolds in vitro. Mater Lett. 2009;63:2313–6.
48. Ngiam M, Liao SS, Patil AJ, Cheng ZY, Chan CK, Ramakrishna S. The fabrication of nano-hydroxyapatite on PLGA and PLGA/collagen nanofibrous composite scaffolds and their effects in osteoblastic behavior for bone tissue engineering. Bone. 2009;45:4–16.
49. Marzke MW. Bones: structure and mechanics. Am J Hum Biol. 2003;15:464–5.
50. Kim SS, Park MS, Jeon O, Choi CY, Kim BS. Poly(lactide-co-glycolide)/hydroxyapatite composite scaffolds for bone tissue engineering. Biomaterials. 2006;27:1399–409.
51. Lee J, Tae G, Kim YH, Park IS, Kim SH, Kim SH. The effect of gelatin incorporation into electrospun poly(L-lactide-co-epsilon-caprolactone) fibers on mechanical properties and cytocompatibility. Biomaterials. 2008;29:1872–9.
52. Tan HP, Wu JD, Lao LH, Gao CY. Gelatin/chitosan/hyaluronan scaffold integrated with PLGA microspheres for cartilage tissue engineering. Acta Biomater. 2009;5:328–37.
53. Liao SS, Cui FZ, Zhu Y. Osteoblasts adherence and migration through three-dimensional porous mineralized collagen based composite: nHAC/PLA. J Bioact Comp Polym. 2004;19:117–30.
54. Dulgar-Tulloch AJ, Bizios R, Siegel RW. Human mesenchymal stem cell adhesion and proliferation in response to ceramic chemistry and nanoscale topography. J Biomed Mater Res A. 2009;90A:586–94.
55. Cui Y, Liu Y, Cui Y, Jing XB, Zhang PBA, Chen XS. The nanocomposite scaffold of poly(lactide-co-glycolide) and hydroxyapatite surface-grafted with L-lactic acid oligomer for bone repair. Acta Biomater. 2009;5:2680–92.
56. Tsukamoto Y, Fukutani S, Mori M. Hydroxyapatite-induced alkaline-phosphatase activity of human pulp fibroblasts. J Mater Sci Mater Med. 1992;3:180–3.
57. Gupta D, Venugopal J, Mitra S, Dev VRG, Ramakrishna S. Nanostructured biocomposite substrates by electrospinning and electrospraying for the mineralization of osteoblasts. Biomaterials. 2009;30:2085–94.